[CANCER RESEARCH 59, 3682–3688, August 1, 1999]

Enhanced Amsacrine-induced Mutagenesis in Plateau-Phase Chinese Hamster Ovary Cells, with Targeting of +1 Frameshifts to Free 3′ Ends of Topoisomerase II Cleavable Complexes[1]

Kathleen Patteson, Peng Wang, and Lawrence F. Povirk[2]

Department of Pharmacology and Toxicology, Medical College of Virginia, Virginia Commonwealth University, Richmond, Virginia 23298

ABSTRACT

Previous work showed that the DNA double-strand cleaving agents bleomycin and neocarzinostatin were more mutagenic in plateau-phase than in log-phase cells. To determine whether topoisomerase II poisons that produce double-strand breaks by trapping of cleavable complexes would, likewise, induce mutations specific to plateau-phase cells, *aprt* mutations induced by amsacrine in both log-phase and plateau-phase CHO cells were analyzed. The maximum *aprt* mutant frequencies obtained were 7×10^{-6} after treatment with 0.02 μM amsacrine in log phase and 27×10^{-6} after treatment with 1 μM amsacrine in plateau phase, compared with a spontaneous frequency of $<1 \times 10^{-6}$. Base substitutions dominated the spectrum of mutations in log-phase cells, but were much less prevalent in plateau-phase cells. Both spectra also included small deletions, insertions and duplications, as well as few large-scale deletions or rearrangements. About 5% of the log-phase mutants and 16% of the plateau-phase mutants were +1 frameshifts, and all but one of these were targeted to potential free 3′ termini of cleavable complexes, as determined by mapping of cleavage sites in DNA treated with topoisomerase II plus amsacrine *in vitro*. Thus, these insertions may arise from templated extension of the exposed 3′ terminus by a DNA polymerase, followed by resealing of the strand, as shown previously for acridine-induced frameshifts in T4 phage.

INTRODUCTION

The cleavable complex of topoisomerase II is an intermediate in strand passage wherein the two strands of a DNA duplex have been cleaved, on a four-base 5′ stagger. The 3′ termini of the breaks are free hydroxyls, but each 5′ terminus is covalently bound to a topoisomerase II subunit, and the two DNA ends are held together by interactions between two such subunits. Many topoisomerase-based cancer chemotherapeutic agents effect cell killing by trapping this cleavable complex intermediate and preventing religation of the DNA strands. This trapping can result in disruption of DNA metabolism, particularly the decatenation and separation of sister duplexes after replication, or can lead, by an unknown process, to irreversible double-strand breaks (1–4).

At sublethal concentrations, topoisomerase inhibitors that stabilize the cleavable complex are potent mutagens, but the spectrum of the recovered mutations depends strongly on the nature of the genetic locus examined (5–7). At heterozygous loci in mammalian cells (as typified by the $TK^{\pm}$ assay), these agents can produce specific-locus mutant frequencies as high as several percent, and most of the mutations are very large multilocus deletions (8, 9). However, at the hemizygous *aprt*[3] locus of CHO-D422 cells, where such large deletions would be lethal, mutant frequencies are much lower, and smaller deletions and insertions (usually <20 bp), as well as base substitutions, become dominant. The small deletions induced by the nonintercalating topoisomerase II inhibitor teniposide in this system seemed to be targeted to potential sites of cleavable complex formation, but the exact positioning of the deletion end points with respect to the potential cleavage sites was highly variable, suggesting somewhat complex processing of the DNA ends before religation (10).

In T4 phage, intercalating topoisomerase II inhibitors such as 9-aminoacridine, proflavine, and the cancer chemotherapeutic agent amsacrine (*m*-AMSA), are potent frameshift mutagens, producing predominantly +1, +2, and −1 frameshifts that are targeted to hotspots of cleavable complex formation. These frameshifts are almost always positioned such that they can be explained by removal or templated addition of one to two nucleotides at the exposed 3′ DNA termini of the cleavable complexes (11), presumably by T4 DNA polymerase and its potent associated 3′→5′ exonuclease (12). The apparent low frequency of such events among mutations induced by the nonintercalating inhibitor teniposide in CHO cells (10) raises the question of whether such frameshifts might be induced only by intercalating inhibitors or, alternatively, might result from unique features of DNA processing in T4.

This and certain other proposed mechanisms of mutagenesis by these agents (most notably, misrepair of double-strand breaks; ref. 10) do not involve replicative DNA synthesis, raising the possibility that mutations could be induced even in nonproliferating cells. Indeed, we previously reported that two free radical-based DNA double-strand cleaving agents, bleomycin and neocarzinostatin, were significantly mutagenic only in confluence-arrested cells (13, 14).

To address both these questions, *aprt* mutations induced by treatment with *m*-AMSA in both log- and plateau-phase CHO cells were analyzed.

MATERIALS AND METHODS

Mutagenesis and Sequencing For plateau-phase treatment, 1000-cell inocula were grown to confluent monolayers in 6-well plates, as described (13), and treated with *m*-AMSA for 2 days, with fresh, drug-containing conditioned medium added every 12 h. The cells were then trypsinized, and an aliquot was plated at low density to assess clonogenic survival. The bulk of the cells were released into exponential growth for 6 days, and then a total of 2.5×10^6 cells were plated in the presence of 0.4 mM 8-azaadenine to select *aprt* mutants (10).

For log-phase treatment, 5×10^5 cells grown from a 1000-cell inoculum were seeded into a 75-cm^2 tissue culture flask. After incubation for 24 h, they were treated with *m*-AMSA for 16 h, and survival and mutagenesis were assessed as above (10).

Individual mutant colonies were recovered by trypsinization in cloning rings, and expanded to $\sim 10^7$ cells for automated DNA extraction (program 163; Autogen Instruments, Framingham, MA). Coding portions of *aprt* were amplified by PCR in two segments comprising either exons 1 and 2 or exons 3–5, and each exon was sequenced (10). Mutants lacking one or both products were subjected to PCR with additional primers within and flanking *aprt* to localize the sequence alteration (14). Mutants with no alterations in *aprt* exons were, likewise, subjected to additional PCR to screen for possible rearrangements in the large intron 2. No more than two mutants were selected from each treated culture; in cases where the two clones had identical mutations, they were assumed to have arisen from a single mutational event, and that mutation was counted only once in the data analysis.

Mapping of Topoisomerase Cleavage Sites *in Vitro*. Cloned, 5′-end-labeled fragments containing each of the *aprt* exons were prepared as described previously (14). Labeled fragments (~ 0.2 μg) were treated with 4 units of human

Received 1/25/99; accepted 6/3/99.

The costs of publication of this article were defrayed in part by the payment of page charges. This article must therefore be hereby marked *advertisement* in accordance with 18 U.S.C. Section 1734 solely to indicate this fact.

[1] Supported by Grant CA40615 from the NIH, Department of Health and Human Services.

[2] To whom requests for reprints should be addressed, at Department of Pharmacology and Toxicology, Medical College of Virginia, P. O. Box 980230, 1101 East Marshall Street, Richmond, VA 23298-0230. Phone: (804) 828-9640; E-mail: LPOVIRK@gems.vcu.edu.

[3] The abbreviations used are: *aprt*, adenine phosphoribosyltransferase; *m*-AMSA, (4′-(9-acridinylamino)methanesulfon-*m*-anisidide; CHO, Chinese hamster ovary.

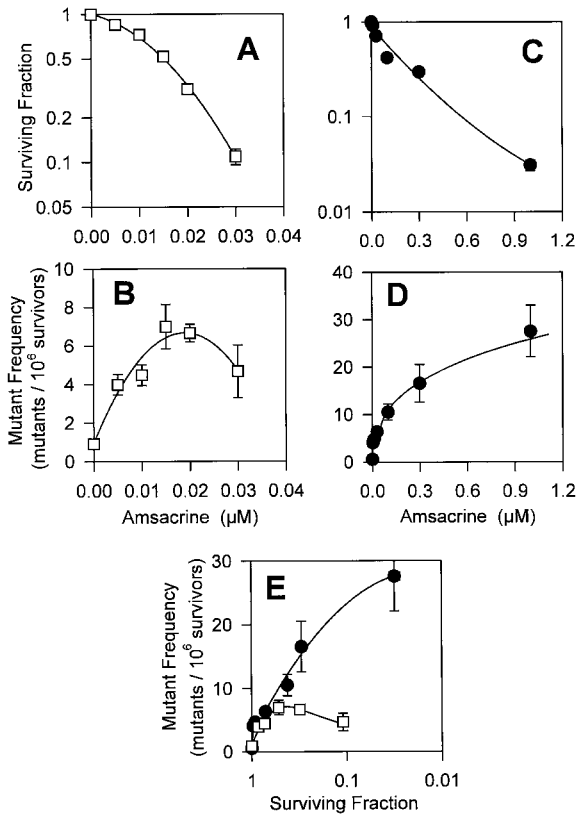

Fig. 1. Mutagenesis and cytotoxicity dose responses for CHO cells treated with *m*-AMSA in log phase (*A* and *B*) or in plateau phase (*C* and *D*). To compare the mutagenic effects at equitoxic doses, mutant frequency in log-phase (□) or plateau-phase (●) cells was plotted as a function of survival (*E*). For log-phase cells, each point is the average ± SE of data from 12–17 independent treated cultures, except for the 0 ($n = 34$) and 0.02 μM ($n = 27$) doses, from a total of 17 experiments. For plateau-phase cells, 0 dose ($n = 20$) and all other doses ($n = 10$), from a total of 10 experiments.

topoisomerase IIα (p170 form; Topogen, Columbus, OH) at 37°C for 10 min in 20 μl of the buffer provided by the vendor [50 mM Tris-Cl (pH 8.0), 120 mM KCl, 10 mM $MgCl_2$, 0.5 mM ATP, 0.5 mM DTT, and 30 μg/ml BSA] plus 10 μM or 20 μM *m*-AMSA. (Previous experiments with other fragments have indicated that the cleavage specificity of the human enzyme is indistinguishable from that of the rodent enzyme, purified from murine L1210 cells and provided by Y. Pommier, National Cancer Institute). Cleavable complexes were trapped with SDS plus proteinase K, and the DNA was phenol-extracted, precipitated, and analyzed on 7% denaturing polyacrylamide gels (10).

Site-specific cleavage was quantitated by phosphorimage analysis using ImageQuant 2.0 software (Molecular Dynamics, Sunnyvale, CA) and was normalized as follows. First, the phosphorimage intensity in each lane was transformed into a line graph. For each sample treated with topoisomerase plus *m*-AMSA, the region of the graph containing fragments resulting from cleavage within the exon was determined by reference to Maxam-Gilbert sequencing markers. The total integrated phosphorimage intensity in this region was calculated, and after subtraction of the intensity in the same area of the control lanes (average of the *m*-AMSA-only and topoisomerase-only samples), it was divided by the number of bp in the exon to give the average frequency of *m*-AMSA- and topoisomerase-dependent cleavage per base within that exon, expressed as phosphorimage intensity. The intensity of each individual band that seemed significantly stronger in the topoisomerase+*m*-AMSA-treated samples was then determined and, after subtraction of the intensity of any detectable band at the same position in the control lanes, was divided by the average cleavage per bp, to give a dimensionless quantity representing the relative cleavage frequency at each site, as compared with an "average" base position in that exon (14). Any base position with a relative cleavage frequency >1.0 was considered to be a cleavage site.

Statistics. The statistical significance of the apparent targeting of mutations to certain sequence positions was determined from the goodness-of-fit statistic (15) for 2 × 2 tables in which the classification of the observed mutation sites according to a given criterion was compared with the classification of all sequence positions in *aprt* exons according to the same criterion. In the specific case of +1 frameshifts, each observed frameshift was classified on the basis of whether it was consistent with duplication of a base at the 5′ terminus of a site for cleavage by *m*-AMSA plus topoisomerase II *in vitro*; for comparison, each base in all *aprt* exons was classified on the basis of whether duplication of that base would be indistinguishable from duplication of a 5′ terminal base at a cleavage site. For example, in the sequence . . . TCC↓CCA. . . (where "↓" represents a cleavage site), a +1 duplication to give . . . TCCCCCA. . . would be considered to be targeted to that cleavage site, but all four Cs in the sequence would have to be classified as potential target sites in the calculation.

The significance of differences between spectra was assessed by Monte Carlo simulations of the appropriate 2 × *N* tables, where *N* is the number of mutant categories (16). To assess differences in a particular category of mutant, all other categories were combined and the *P* for the resulting 2 × 2

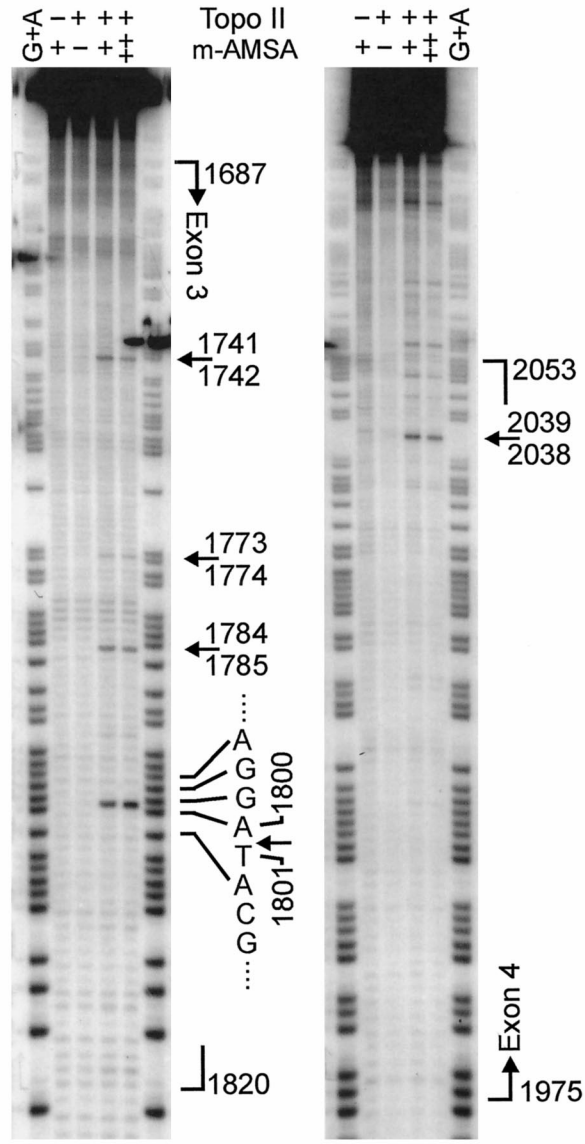

Fig. 2. DNA cleavage by topoisomerase II plus 10 μM (+) or 20 μM (++) *m*-AMSA in the transcribed strand of exon 3 (*A*) and in the coding strand of exon 4 (*B*). *Arrows*, the positions of prominent cleavage sites. *Lowest arrow* in *A* shows cleavage corresponding to the +1 frameshift hotspot at bp 1800. (The band corresponding to topoisomerase-mediated cleavage between A_{1800} and T_{1801} is a fragment with the 3′ terminal structure . . . $GCAT_{OH}$; this species migrates ~1/2 nucleotide position more slowly than the Maxam-Gilbert marker for A_{1800}, which has terminal structure . . . GCATp.) The single strongest cleavage site in *aprt* was at bp 2038–2039 in the coding strand of exon 4, as shown in *B*. *Brackets*, the extent of exons in the sequence, with the *large arrow* showing the direction of transcription.

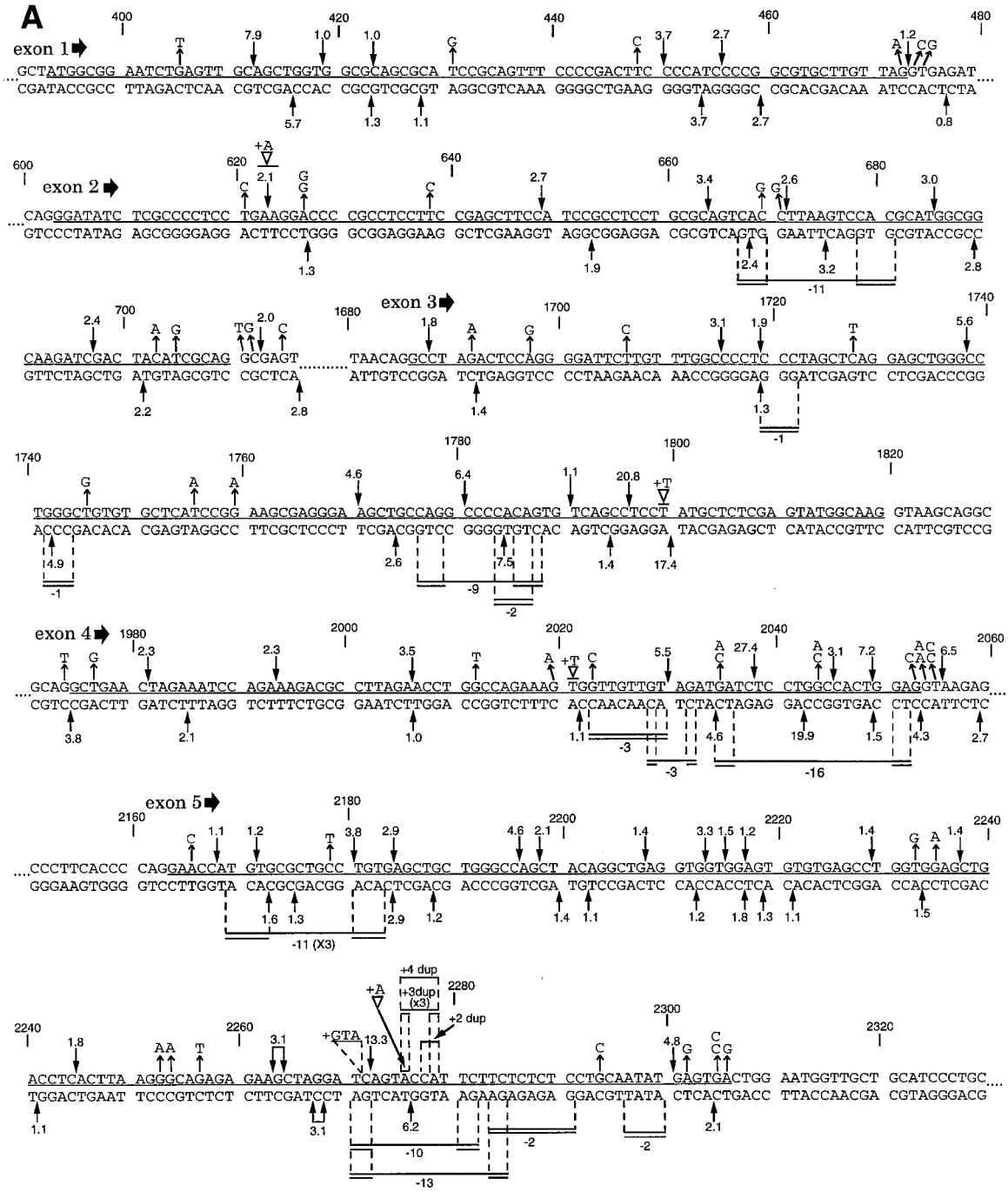

Fig. 3. Mapping of cleavable complex sites and *m*-AMSA-induced mutations in *aprt* exons for cells treated in log phase (*A*) or in plateau phase (*B*). Exons are *underlined*. *Arrows* facing toward the sequence show cleavage sites in each strand as detected *in vitro*, with numbers indicating relative cleavage intensity normalized to the average cleavage frequency per base in each strand of each exon (average of the 10 μM and 20 μM m-AMSA treatments; see Fig. 2). Only sites with relative cleavage frequencies >1 are shown. *Arrows* facing away from the sequence show base substitutions, in terms of the top (coding) strand. Above the sequence: ▽, single-base duplications (+1 frameshifts); *horizontal lines*, larger duplications (dup). *Double-lined segments* indicate that the exact position of the duplication was indeterminate, either because it occurred within a tandem repeat or because there were repeated base(s) at both the beginning and the end of the duplicated segment. Numbers above the line indicate the net number of bp added, and "×3" indicates that the same mutation was recovered from three independently treated cultures. *Horizontal lines* and numbers below the sequence indicate the position and size of induced deletions. *Double lines* at each end indicate short direct repeats, one copy of which was retained in the mutant sequence. *Double lines* spanning the entire segment indicate deletion of one or more copies of a tandemly repeated sequence, with the net decrease in bp indicated. Numbering of *aprt* sequence positions follows the convention of Phear *et al.* (19), wherein bp 1 corresponds to an upstream *Bam*HI site, and the translation start site is at bp 394. [Note that an alternative numbering convention, with bp 1 at the translation start site (34), was used in some of our earlier work.]

table was multiplied by the number of hypotheses tested, in this case equal to the number of categories *N*.

RESULTS

Mutagenesis and Cell Killing in Log and Plateau Phases. In exponentially growing CHO cells, the survival and mutagenesis responses were qualitatively similar to those reported previously for teniposide, a nonintercalating but otherwise functionally similar topoisomerase II poison (10). Significant mutagenesis was seen even at >90% survival, but the mutant frequency quickly leveled off at about 7×10^{-6}/survivor (eight times background), and seemed even to decrease slightly at the highest dose (Fig. 1, *A* and *B*).

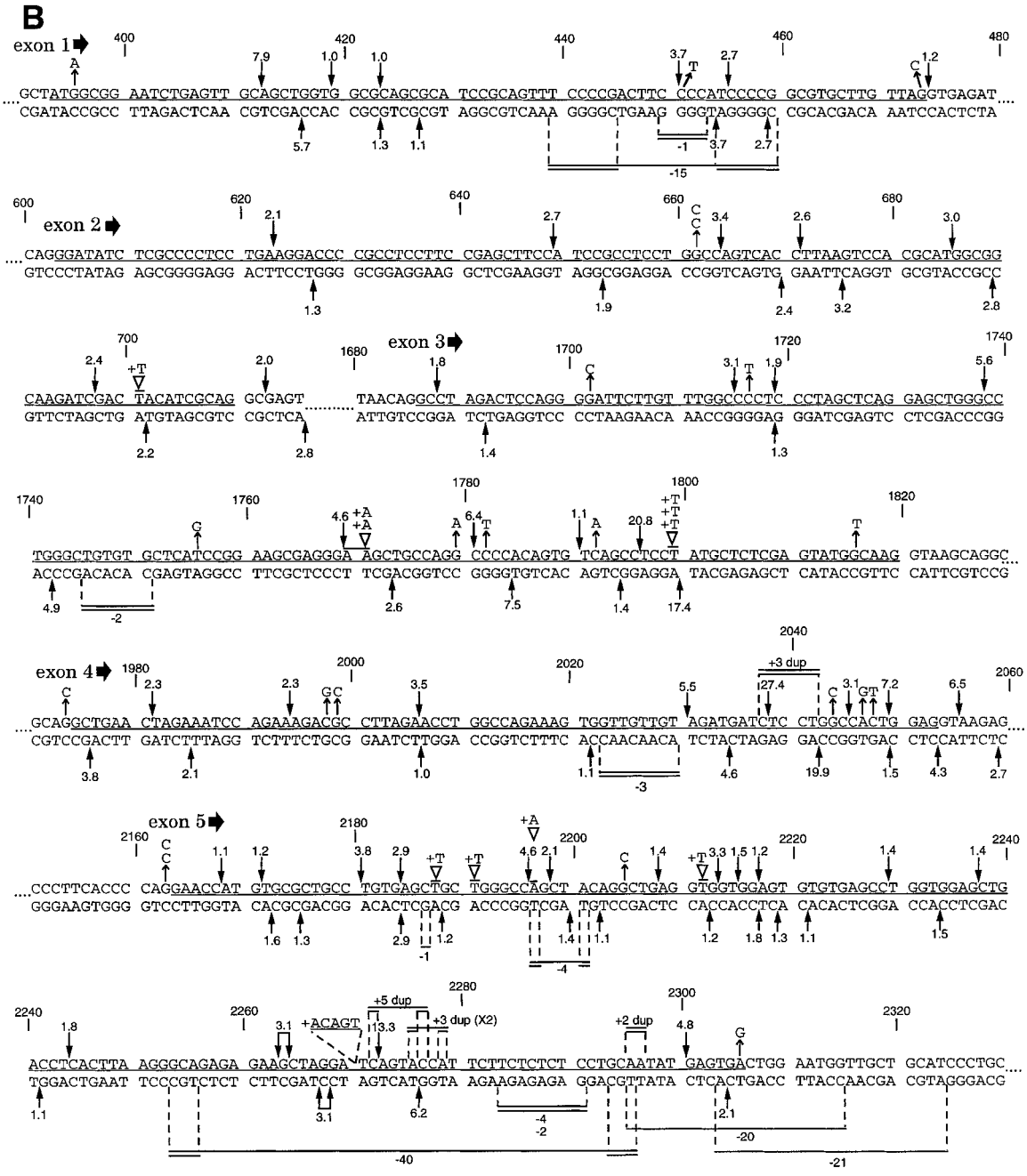

As expected from the known down-regulation of topoisomerase II in plateau phase (17), *m*-AMSA was about 10-fold less cytotoxic to plateau-phase cells, although the treatment time was 3-fold longer. At very low *m*-AMSA concentrations, the mutant frequencies in log- and plateau-phase cells were similar (*e.g.*, 4.5 *versus.* 4.1 $\times$ 10^{-6} at 0.01 μM). However, in plateau-phase cells, the mutant frequency continued to increase with drug concentration, reaching nearly 3 $\times$ 10^{-5} at the highest dose where mutagenesis could still be assayed (Fig. 1, *C-E*). This response was more similar to that seen for the radiomimetic DNA-cleaving agents bleomycin and neocarzinostatin, in plateau-phase cells (13, 14).

Distribution of Mutation Types Except for the presence of several large-scale deletions/rearrangements, the spectrum of *m*-AMSA-induced mutations in log-phase cells was similar to that of spontaneous mutations and included base substitutions as well as small deletions, insertions, and duplications (Table 1). However, in addition to large-scale rearrangements, *m*-AMSA treatment of plateau-phase cells resulted in a relative decrease in the proportion of base substitutions ($P < 0.002$) and an increase in +1 frameshifts ($P < 0.05$). Also, among the base substitutions from cells treated in plateau phase, an unusually high proportion were G•C→C•G transversions (11 of 22 as compared with 3 of 17 spontaneous substitutions). However, there was no apparent targeting of the base substitutions to sites of cleavable complexes. Contrary to the spectrum of base substitutions in lymphocytes of patients treated with the nonintercalating topoisomerase II inhibitor etoposide (18), there was no apparent increase in A•T→T•A transversions as a result of *m*-AMSA treatment of CHO cells. To assess possible differences between mutants induced by treatment with different concentrations of *m*-AMSA, each spectrum was partitioned into high- and low-dose spectra with approximately equal numbers of mutants in each (data not shown); no significant dose-dependent differences were found ($P > 0.25$ in both cases).

Mapping of Cleavable Complex Sites *in Vitro*. To evaluate specific hypotheses concerning the role of cleavable complexes in me-

diating various *m*-AMSA-induced mutations, it was necessary to determine the sites in *aprt* at which cleavable complexes would form. Therefore, cleavable complexes in end-labeled *aprt* DNA fragments treated with topoisomerase plus *m*-AMSA were trapped with detergent, and the cleavage sites were mapped at single-nucleotide resolution (Fig. 2). Except for a few of the weakest sites, nearly all of the detected cleavage sites were paired in opposite strands on a four-base stagger (Fig. 3), as expected for cleavage of both strands in a single cleavable complex (1–3). Furthermore, the two sites in a given pair usually showed similar cleavage intensities. There were two predominant cleavage hotspots, one at bp 1797–1800 in exon 3 and one at bp 2039–2042 in exon 4 (Fig. 2). Cleavage at these sites was ~20-fold greater than the average cleavage frequency/bp and about twice as great as at any other sites in the *aprt* exons (Fig. 3).

Targeting of +1 Frameshifts to Cleavable Complexes. Frameshifts corresponding to duplications of a single bp accounted for 5% of log-phase and 16% of plateau-phase *m*-AMSA-induced mutations, a total of 14 independent mutations. Nearly all of these (4 of 4 log-phase and 9 of 10 plateau-phase mutants; ▽ in Fig. 3) occurred precisely at the cleavage sites of cleavable complexes, as detected in *aprt* DNA *in vitro*. In every case, the frameshift could be described as a duplication of the base at the 5′ terminus of the transient, topoisomerase II-mediated break, consistent with a model involving polymerase-catalyzed, templated addition of a single nucleotide to the free 3′ end of the break, followed by resealing of the break (11). One of the two predominant hotspots for *m*-AMSA-induced cleavage in *aprt* (at bp 1800; see Fig. 2*A*) was also a frameshift hotspot, accounting for one log-phase and three plateau-phase +1 frameshifts. Because there are only 116 sequence positions in *aprt* exons at which a single-base duplication would be indistinguishable from duplication of a 5′-terminal base at a cleavage site, the fraction of +1 frameshifts positioned at potential cleavage sites is much greater than would be expected on the basis of chance (13 of 14 *versus* 116 of 543; $P < 10^{-7}$). Several of the slightly larger duplications (*e.g.*, +3 at bp 2037–2042 and +5 at bp 2272–2277; see Fig. 3*B*) were also consistent with templated addition at free 3′-ends of topoisomerase II cleavable complexes. However, there were also several duplications (including the +3 duplication hotspot at bp 2276–2279) that did not conform to the templated extension model.

Other Mutations. Small deletions were similar in log- and plateau-phase cells and ranged from 1–40 bp. Slightly less than half of these were deletions of one repeat unit in tandem singlet, doublet, or triplet repeats (*e.g.*, shortening of the tandem triplet repeat GTTGTTGT at bp 2023–2030 to GTTGT; Fig. 3). The tandem deletions did not seem to be targeted to cleavable complexes. There were also several small insertions that were duplications of one repeat unit in similar tandem repeats (double lines above the sequence in Fig. 3). Nearly all (8 of 10) *m*-AMSA-induced duplications were associated with the prominent potential cleavage site at bp 2273–2276, which also lies within the stem of a large potential cruciform structure (19) spanning bp 2269–2326. Two additional insertions could be described as imperfect duplications of adjacent sequences [*i.e.*, insertion of GTA immediately preceding CAGTA at bp 2272 (Fig. 3*A*) and insertion of ACAGT preceding TCAGT at bp 2271 (Fig. 3*B*)].

The other, nontandem deletions were slightly larger, predominantly between 9 and 21 bp, and were usually marked by 1–6 bp repeats at the deletion end points. Although these deletions often encompassed prominent potential cleavable complex sites (Figs. 3 and 4) and the average cleavage frequency within the deleted sequences was 2.5 times higher than that in sequences not involved in any deletion (data not shown), this apparent correspondence was not statistically significant.

Attempts to sequence the large-scale rearrangements are in progress. As reported previously, one of these was an apparent topoisomerase II subunit exchange event resulting in a precise reciprocal chromosomal translocation, without loss of even a single bp of sequence (20). However, mapping data obtained thus far (data not shown) indicate that most or all of the remaining rearrangements are accompanied by loss of large segments of *aprt*, although none of them seem to have lost the entire gene.

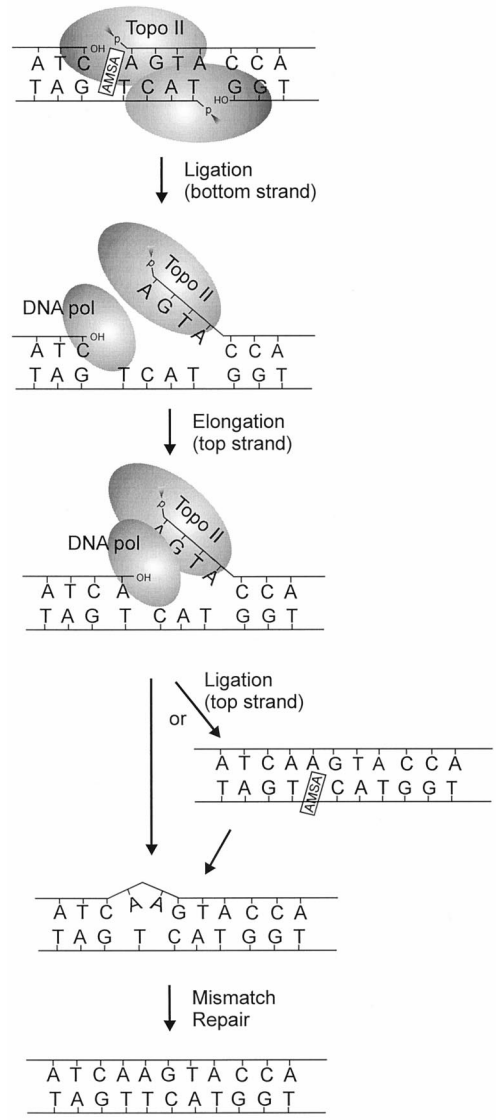

Fig. 4. Model for *m*-AMSA-induced +1 frameshifts, adapted from Ripley *et al.* (11). A single nucleotide is added by a DNA polymerase to a free 3′-hydroxyl terminus in an *m*-AMSA-stabilized cleavable complex. The break is then resealed by topoisomerase II, resulting in duplication of the base at the 5′ end of the break. The branched pathway shows the possible stabilization of the mismatched ligation substrate by *m*-AMSA intercalation into one strand. Although the model shows transient breaks in both strands, it does not exclude the possibility of a break in the top strand only.

For log-phase cells, the proportion of 8-azaadenine-resistant clones having no detectable alteration in the *aprt* gene was comparable with that reported for other mutagens, but for plateau-phase cells, the proportion of such clones was unusually high, about 16%. Although these clones were not further characterized, they are reminiscent of the 25% of *m*-AMSA-induced 6-thioguanine-resistant clones of AS52 cells (putative *gpt* mutants) in which the *gpt* coding sequence and promoter remained unaltered, but in which there were large-scale rearrangements in the vicinity of *gpt*, as well as reduced *gpt* expression (7). The results in both systems could be explained by rearrangements that translocate the entire, intact *aprt* or *gpt* gene into a genomic region with a chromatin structure that suppresses transcription.

Table 1 *Distribution of mutation types in m-AMSA-treated cells*

The proportions of each type of mutation recovered from m-AMSA-treated cells are compared with those for untreated cells (Refs. 10, 13, 14, and 25). Mutants were collected from the same experiments used to generate the dose response curves (Fig. 1), with one or two mutants recovered from each treated culture. The average m-AMSA-induced increase in mutant frequency was 6.4-fold for log-phase cells and 27-fold for plateau-phase cells. In all of the spectra, every base substitution reflected a predicted amino acid or splice junction change (data not shown).

	Untreated Cells		m-AMSA-treated cells	
	Log-phase *n* (%)	Plateau-phase *n* (%)	Log-phase *n* (%)	Plateau-phase *n* (%)
Base substitutions	27 (63)	26 (72)	50 (57)	22 (34)
−1 frameshifts	3 (7)	2 (6)	2 (2)	3[a] (5)
+1 frameshifts	1 (2)	0 (0)	4 (5)	10 (16)
Small deletions				
Tandem	0 (0)	2 (6)	4 (5)	4 (6)
Nontandem	7 (16)	4 (11)	9 (10)	5 (8)
Duplications/insertions	2 (5)	0 (0)	6 (7)	6 (9)
Large-scale deletions/ rearrangements	0 (0)	0 (0)	8 (9)	4 (6)
No change	3 (7)	2 (6)	5 (6)	10 (16)
Total[b]	43 (100)	36 (100)	88 (100)	64 (100)

[a] Includes an ACCA→AAA sequence change at bp 2276–2279; not shown in Fig. 3.
[b] Includes 8-azaadenine-resistant clones in which no alteration in the *aprt* gene was detected.

DISCUSSION

At most genetic loci, including the *tk* locus in mouse lymphoblasts (9), the integrated *Escherichia coli gpt* gene in CHO-AS52 cells (7), and the functionally hemizygous X-linked *HPRT* locus in several cell lines (5, 6, 21), *m*-AMSA and other topoisomerase inhibitors induce primarily large-scale deletion and rearrangement mutations. Although these mutations presumably result from cellular processing of cleavable complexes, the exact mechanisms of their formation are not known. Very few of these large-scale mutations have been analyzed at the sequence level, and it is, thus, difficult to distinguish between topoisomerase subunit exchange mechanisms and models involving more complex processing and joining of broken DNA ends.

The hemizygous *aprt* locus in CHO-D422 cells is a rather special case in that the gene is unusually small (~2 kb) and is flanked downstream by an apparently essential intracisternal-A particle gene (22). This feature dramatically decreases the incidence of viable deletion mutants by constraining the downstream breakpoint to a region of a few thousand bp. Thus, point mutations and smaller deletions/insertions that might be rare in other systems (7) tend to dominate *aprt* mutation spectra, even for highly clastogenic agents such as X-rays (23), radiomimetic drugs (13, 14), and topoisomerase inhibitors (10), making *aprt* ideally suited for elucidating the mechanisms of these small-scale genetic alterations.

The most unusual feature of the spectrum of *m*-AMSA-induced *aprt* mutations in CHO-D422 cells is the presence of a number of +1 frameshifts, invariably reflecting duplication of a single bp in the sequence. Among spontaneous *aprt* mutations, +1 frameshifts are extremely rare, accounting for only one of over 200 such mutations that have been sequenced by various laboratories (10, 14, 19, 24, 25). The bases duplicated in most of the *m*-AMSA-induced +1 frameshifts were flanked on both sides by nonidentical bases, suggesting that they could not be accounted for by the replication slippage mechanisms often invoked to explain frameshift mutations (26). Most strikingly, 13 of the 14 *m*-AMSA-induced +1 frameshifts were consistent with duplication of a base at the 5′ terminus of a cleavage site in a potential topoisomerase II cleavable complex, a correlation far greater than would be expected from random positioning of these mutations ($P < 10^{-7}$). This is the same pattern reported previously for acridine-induced +1 frameshifts in T4 phage and is precisely the result predicted by a model involving polymerase-catalyzed extension of the exposed 3′ terminus, followed by religation of the break (11). Thus, it seems highly likely that the *m*-AMSA-induced frameshifts in CHO cells arise by an identical mechanism (Fig. 4). As has been noted previously (11), inhibitor data suggest that the topoisomerase II of T4 may be quite similar to the mammalian enzyme; certainly more similar than is, for example, *E. coli* gyrase.

However, in the T4 system, an almost equal number of acridine-induced −1 frameshifts, invariably reflecting loss of a base at the 3′ terminus of a cleavable complex, were also detected, and these have been attributed to removal of a single base by the potent 3′→5′ exonuclease of T4 polymerase, followed by ligation (11). In further support of this model, the prevalence of acridine-induced −1 frameshifts is increased in T4 strains having enhanced polymerase-associated exonuclease activity, and is reduced in strains having reduced exonuclease activity (12). Thus, the near absence of *m*-AMSA-induced −1 frameshifts in CHO *aprt* is most easily explained by the mammalian DNA polymerase having a less potent associated exonuclease.

A critical question with regard to the model in Fig. 4 is the exact mechanism by which religation is effected, whether by topoisomerase II, by DNA ligase (after removal of topoisomerase II), or by some more complex pathway. *In vitro* studies have shown that *Drosophila* topoisomerase II can form relatively stable cleavable complexes by reaction with single-stranded circular DNA and that these complexes can then react with oligomeric DNA duplexes bearing either blunt or staggered ends, resulting in ligation of the 5′ end of the linearized circle to the oligomer (27). This result indicates that a continuous DNA duplex is not absolutely required either to maintain reversibility of the cleavage/religation reaction, or to allow the religation. Thus, these results support at least the plausibility of the scheme shown in Fig. 4, with religation effected by topoisomerase.

A second question is whether *m*-AMSA intercalation, in addition to stabilizing the cleavable complex, might also act to stabilize a DNA duplex with a frameshift mismatch (presumably by intercalation into one strand only) and, thus, facilitate religation of the mismatched duplex. In certain systems that lack an acridine-sensitive type II topoisomerase (28), acridines induce +1 and −1 frameshifts in monotonous base runs, a result that tends to confirm the possibility that a frameshift-mismatched duplex might be stabilized by acridine intercalation into one strand. Likewise, the finding (10) that not a single +1 frameshift consistent with the model in Fig. 4 was detected among *aprt* mutations generated in log-phase CHO-D422 cells by teniposide (a nonintercalating but otherwise functionally similar topoisomerase II inhibitor) also suggests that *m*-AMSA intercalation may play some role in addition to merely stabilizing cleavable complexes. Admittedly, however, the number of +1 frameshifts involved is small (4 of 88 *m*-AMSA-induced *versus* 0 of 68 teniposide-induced mutations, in log-phase cells; $P \sim 0.13$). (There are no data available on this question from the T4 system because T4 topoisomerase is insensitive to teniposide.)

The origins of other types of m-AMSA-induced *aprt* mutations are less clear. The present comparison of log- *versus* plateau-phase mutants was conducted partly as an attempt to determine whether certain types of mutations might be formed by replication-independent mechanisms. Although cells treated in plateau phase must eventually proliferate to allow detection of the mutants, it is expected that very few cleavable complexes will remain by the time the cells progress through S phase because m-AMSA-induced complexes are known to reverse rapidly on drug removal (29). Thus, the finding that mutant frequencies (with the possible exception of base substitutions) are much higher for cells treated in plateau phase suggests that, at least for mutations targeted to cleavable complexes, the conversion of the complexes to permanent DNA sequence changes must occur in G_1/G_0 phase, presumably by mechanisms other than attempted replication of a damaged template. Possible such

mechanisms may include, in addition to that shown in Fig. 1, the conversion of cleavable complexes to frank double-strand breaks, followed by error-prone repair of those breaks by nonhomologous end-joining, leading to small deletions and insertions, as well as large-scale rearrangements. We previously invoked this mechanism to explain the apparent targeting of certain teniposide-induced small deletions and duplications in the *aprt* gene to sites of potential cleavable complex sites. Alternatively, frank breaks, once formed, may persist into S phase and promote deletions, insertions, and rearrangements during replication. Finally, Ripley (30) has proposed that essentially all small deletions and duplication induced in mammalian cells by topoisomerase inhibitors could be accounted for by a single mechanism in which one to several bases are added at the 3′ terminus of a break and/or deleted from the 5′ terminus. Whatever mechanism(s) is responsible, it seems clear that *m*-AMSA is capable of inducing mutations (including, presumably, oncogenic mutations) even in cells that are in a strictly nonproliferative state. Indeed, it may be that in the absence of replication or mitosis, cleavable complexes are still quite mutagenic but much less cytotoxic, thus accounting for the higher levels of mutagenesis achievable in plateau phase. The marked increase in the ratio of topoisomerase IIβ to topoisomerase IIα in plateau phase (31, 32) could conceivably be a factor, as well.

A substantial proportion of the *m*-AMSA-induced *aprt* mutations, in particular the base substitutions and the deletions at tandem repeats, show little, if any, evidence of being targeted to cleavable complexes. These types of mutations are not peculiar to topoisomerase inhibitors but are found in spontaneous mutation spectra, as well (10, 14, 19, 24). Nevertheless, the absolute frequencies of these mutations must be increased by *m*-AMSA treatment; otherwise they would be much less prevalent in spectra of treated cells, given the 6- or 27-fold increase in overall mutant frequency. One possibility is that these apparently untargeted mutations may result from a global decrease in replication fidelity arising, by some unknown mechanism, as a result of drug treatment. It is conceivable that such a loss of fidelity would persist even after the vast majority of drug-stabilized cleavable complexes have religated (33), as would be required to explain the prevalence of these types of mutations in cells treated in plateau phase.

The demonstration of *m*-AMSA-induced +1 insertions targeted to 3′ termini of cleavable complexes may have implications for *m*-AMSA-induced large-scale rearrangements, as well. Specifically, the finding that these 3′ termini can apparently be extended and then religated by topoisomerase II despite the frameshift mismatch in the usual four-base overlap suggests such extensions could also be tolerated in cases where subunits of two cleavable complexes exchange. Thus, contrary to the single apparent *m*-AMSA-mediated reciprocal exchange we have thus far sequenced (20), some such exchanges might show duplication of a base at the newly formed joint, even if the joint was, in fact, formed by subunit exchange, with topoisomerase II effecting the final religation.

REFERENCES

1. Corbett, A. H., and Osheroff, N. When good enzymes go bad: conversion of topoisomerase II to a cellular toxin by antineoplastic drugs. Chem. Res. Toxicol., *6:* 585–597, 1993.
2. Pommier, Y. DNA topoisomerase I and II in cancer chemotherapy: update and perspectives. Cancer Chemother. Pharmacol., *32:* 103–108, 1993.
3. Tewey, K. M., Chen, G. L., Nelson, E. M., and Liu, L. F. Intercalative antitumor drugs interfere with the breakage-reunion reaction of mammalian DNA topoisomerase II. J. Biol. Chem., *259:* 9182–9187, 1984.
4. Chen, M., and Beck, W. T. Differences in inhibition of chromosome separation and G_2 arrest by DNA topoisomerase II inhibitors merbarone and VM-26. Cancer Res., *55:* 1509–1516, 1995.
5. Anderson, R. D., and Berger, N. A. International Commission for Protection Against Environmental Mutagens and Carcinogens. Mutagenicity and carcinogenicity of topoisomerase-interactive agents. Mutat. Res., *309:* 109–142, 1994.
6. Ferguson, L. R., and Baguley, B. C. Mutagenicity of anticancer drugs that inhibit topoisomerase enzymes. Mutat. Res., *355:* 91–101, 1996.
7. Ferguson, L. R., Turner, P. M., Hart, D. W., and Tindall, K. R. Amsacrine-induced mutations in AS52 cells. Environ. Mol. Mutagen., *32:* 47–55, 1998.
8. DeMarini, D. M., Brock, K. H., Doerr, C. L., and Moore, M. M. Mutagenicity and clastogenicity of teniposide (VM-26) in L5178Y/TK ± 3.7.2C mouse lymphoma cells. Mutat. Res., *187:* 141–149, 1987.
9. DeMarini, D. M., Doerr, C. L., Meyer, M. K., Brock, K. H., Hozier, J., and Moore, M. M. Mutagenicity of *m*-AMSA and *o*-AMSA in mammalian cells due to clastogenic mechanism: possible role of topoisomerase. Mutagenesis, *2:* 349–355, 1987.
10. Han, Y-H., Austin, M. J. F., Pommier, Y., and Povirk, L. F. Small deletion and insertion mutations induced by the topoisomerase II inhibitor teniposide in CHO cells and comparison with sites of drug-stimulated DNA cleavage *in vitro*. J. Mol. Biol., *229:* 52–66, 1993.
11. Ripley, L. S., Dubins, J. S., de Boer, J. G., DeMarini, D. M., Bogerd, A. M., and Kreuzer, K. N. Hotspot sites for acridine-induced frameshift mutations in bacteriophage T4 correspond to sites of action of the T4 type II topoisomerase. J. Mol. Biol., *200:* 665–680, 1988.
12. Kaiser, V. L., and Ripley, L. S. DNA nick processing by exonuclease and polymerase activities of bacteriophage T4 DNA polymerase accounts for acridine-induced mutation specificities in T4. Proc. Natl. Acad. Sci. USA, *92:* 2234–2238, 1995.
13. Povirk, L. F., Bennett, R. A. O., Wang, P., Swerdlow, P. S., and Austin, M. J. F. Single base-pair deletions induced by bleomycin at potential double-strand cleavage sites in the *aprt* gene of stationary phase Chinese hamster ovary D422 cells. J. Mol. Biol., *243:* 216–226, 1994.
14. Wang, P., and Povirk, L. F. Targeted base substitutions and small deletions induced by neocarzinostatin at the *APRT* locus in plateau-phase CHO cells. Mutat. Res., *373:* 17–29, 1997.
15. Sokal, R. B., and Rohlf, F. J. *In:* Biometry, p. 549. San Francisco: W. H. Freeman, 1969.
16. Cariello, N. F., Piegorsch, W. W., Adams, W. T., and Skopek, T. R. Computer program for the analysis of mutational spectra: application to p53 mutations. Carcinogenesis (Lond.), *15:* 2281–2285, 1994.
17. Sullivan, D. M., Glisson, B. S., Hodges, P. K., Smallwood-Kentro, S., and Ross, W. E. Proliferation dependence of topoisomerase II-mediated drug action. Biochemistry, *25:* 2248–2256, 1986.
18. Karnaoukhova, L., Moffat, J., Martins, H., and Glickman, B. Mutation frequency and spectrum in lymphocytes of small cell lung cancer patients receiving etoposide chemotherapy. Cancer Res., *57:* 4393–4407, 1997.
19. Phear, G., Armstrong, W., and Meuth, M. Molecular basis of spontaneous mutation at the *aprt* locus of hamster cells. J. Mol. Biol., *209:* 577–582, 1989.
20. Zhou, R-H., Wang, P., Zou, Y., Jackson-Cook, C. K., and Povirk, L. F. A precise interchromosomal reciprocal exchange between hotspots for cleavable complex formation by topoisomerase II in amsacrine-treated CHO cells. Cancer Res., *57:* 4699–4702, 1997.
21. Berger, N. A., Chatterjee, S., Schmotzer, J. A., and Helms, S. R. Etoposide (VP-16–213)-induced gene alterations: potential contribution to cell death. Proc. Natl. Acad. Sci. USA, *88:* 8740–8743, 1991.
22. Davis, R., and Meuth, M. Molecular characterization of multilocus deletions at a diploid locus in CHO cells: association with an intracisternal-A particle gene. Somatic Cell Mol. Genet., *20:* 287–300, 1994.
23. Grosovsky, A. J., de Boer, J. G., de Jong, P. J., Drobetsky, E. A., and Glickman, B. W. Base substitutions, frameshifts and small deletions constitute ionizing radiation-induced point mutations in mammalian cells. Proc. Natl. Acad. Sci. USA, *85:* 185–188, 1988.
24. de Jong, P. J., Grosovsky, E. A., and Glickman, B. W. Spectrum of spontaneous mutation at the *APRT* locus of Chinese hamster ovary cells: an analysis at the DNA sequence level. Proc. Natl. Acad. Sci. USA, *85:* 3499–3503, 1988.
25. Austin, M. J. F., Han, Y-H., and Povirk, L. F. DNA sequence analysis of mutations induced by melphalan in the CHO *aprt* locus. Cancer Genet. Cytogenet., *64:* 69–74, 1992.
26. Streisinger, G., Okada, Y., Emrich, H., Newton, J., Tsugita, A., Terzaghi, E., and Inouye, M. Frameshift mutations and the genetic code. Cold Spring Harbor Symp. Quant. Biol., *31:* 77–84, 1966.
27. Gale, K. C., and Osheroff, N. Intrinsic intermolecular DNA ligation activity of eukaryotic topoisomerase II. Potential roles in recombination. J. Biol. Chem., *267:* 12090–12097, 1992.
28. Skopek, T. R., and Hutchinson, F. Frameshift mutagenesis of λ prophage by 9-aminoacridine, proflavin and ICR-191. Mol. Gen. Genet., *195:* 418–423, 1984.
29. Zwelling, L. A., Michaels, S., Erickson, L. C., Ungerleider, R. S., Nichols, M., and Kohn, K. W. Protein-associated deoxyribonucleic acid strand breaks in L1210 cells treated with the deoxyribonucleic acid intercalating agents 4′-(9-acridinylamino) methanesulfon-m-anisidide and adriamycin. Biochemistry, *20:* 6553–6563, 1981.
30. Ripley, L. S. Deletion and duplication sequences induced in CHO cells by teniposide (VM-26), a topoisomerase II targeting drug, can be explained by the processing of DNA nicks produced by the drug-topoisomerase interaction. Mutat. Res., *312:* 67–78, 1994.
31. Prosperi, E., Sala, E., Negri, C., Oliani, C., Supino, R., Astraldi Ricotti, G. B., and Bottiroli, G. Topoisomerase II α and β in human tumor cells grown *in vitro* and *in vivo*. Anticancer Res., *12:* 2093–2099, 1992.
32. Capranico, G., Tinelli, S., Austin, C. A., Fisher, M. L., and Zunino, F. Different patterns of gene expression of topoisomerase II isoforms in differentiated tissues during murine development. Biochim. Biophys. Acta, *1132:* 43–48, 1992.
33. Chang, W. P., and Little, J. B. Persistently elevated frequency of spontaneous mutations in progeny of CHO clones surviving X-irradiation: association with delayed reproductive death phenotype. Mutat. Res., *270:* 191–199, 1992.
34. de Boer, J. G., Drobetsky, E. A., Grosovsky, A. J., Mazur, M., and Glickman, B. W. The Chinese hamster *aprt* gene as a mutational target. Its sequence and an analysis of direct and inverted repeats. Mutat. Res., *226:* 239–244, 1989.